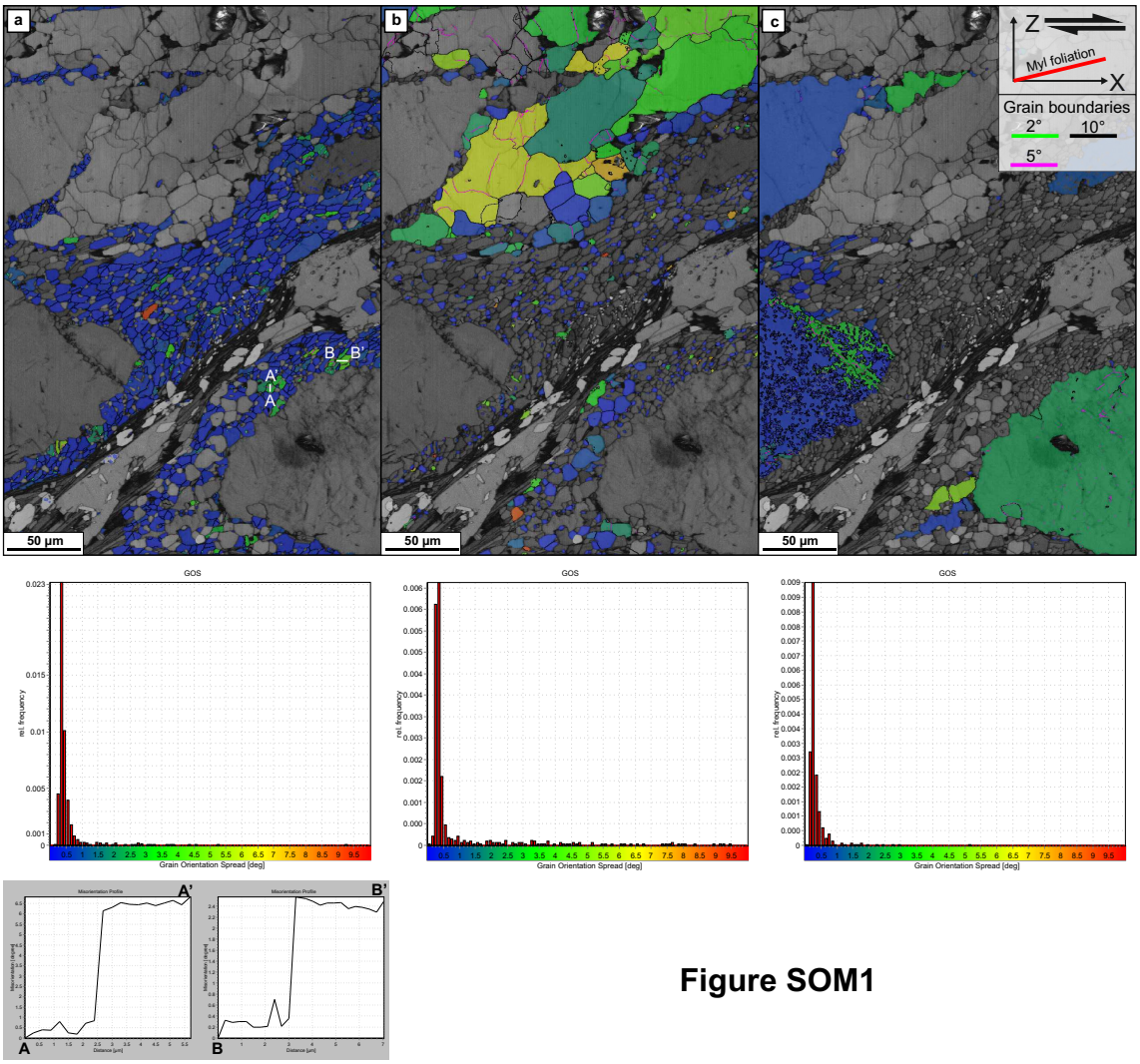
a
b
c
Z
Myl foliation
X
Grain boundaries
2°
10°
5°
B
B'
A'
A
50 µm
50 µm
50 µm
GOS
GOS
GOS
Grain Orientation Spread [deg]
Grain Orientation Spread [deg]
Grain Orientation Spread [deg]
A'
B'
A
B

Figure SOM1

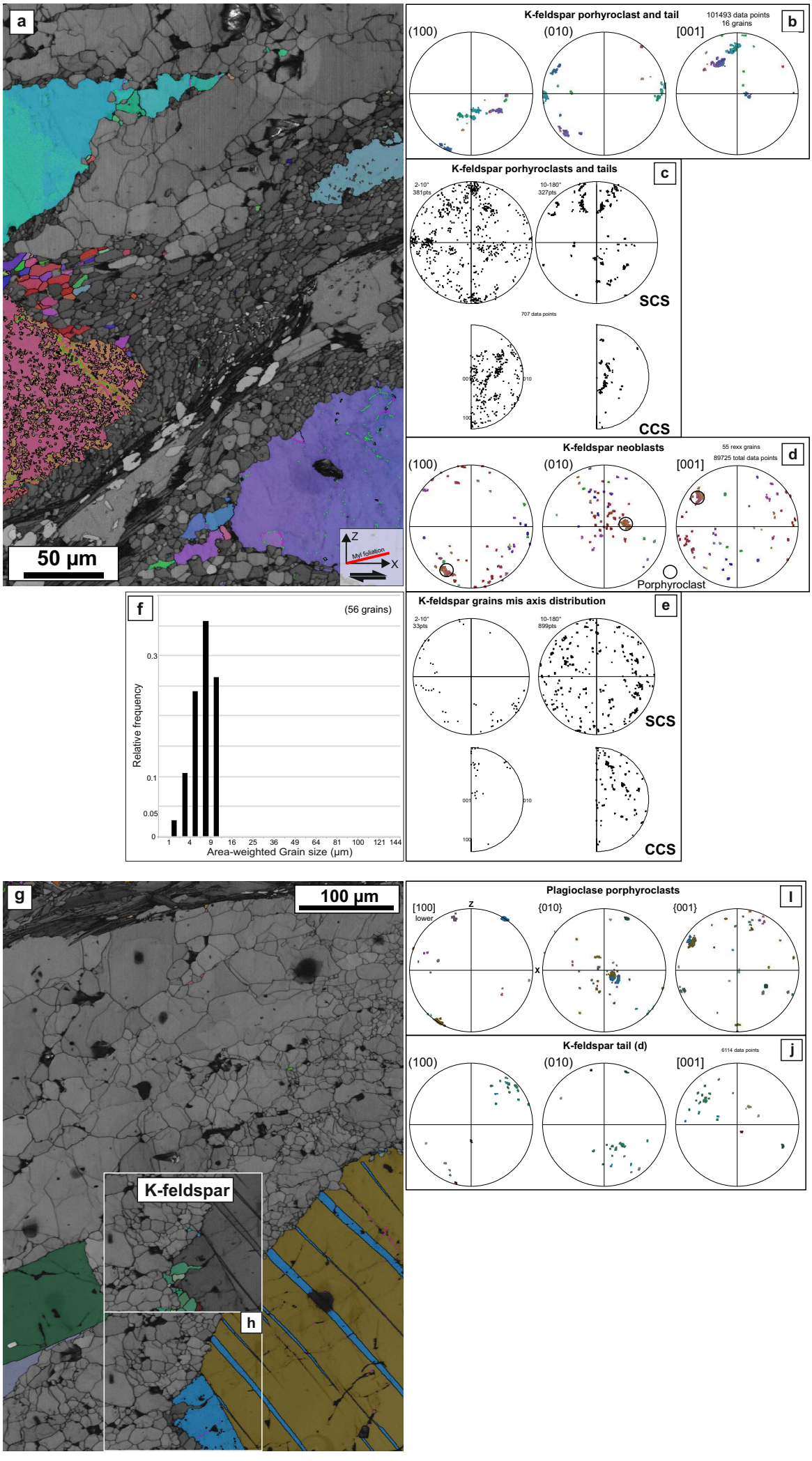
a
50 µm
Z
Myl Foliation
X
K-feldspar porhyroclast and tail
101493 data points
16 grains
b
(100)
(010)
[001]
K-feldspar porhyroclasts and tails
c
2-10°
381pts
10-180°
327pts
SCS
707 data points
CCS
K-feldspar neoblasts
55 rexx grains
89725 total data points
d
Porphyroclast
f
(56 grains)
Relative frequency
0.3
0.1
0.05
0
1 4 9 16 25 36 49 64 81 100 121 144
Area-weighted Grain size (µm)
K-feldspar grains mis axis distribution
e
2-10°
33pts
10-180°
899pts
g
100 µm
K-feldspar
h
Plagioclase porphyroclasts
l
[100]
lower
{010}
{001}
K-feldspar tail (d)
6114 data points
j

Fig. SOM2

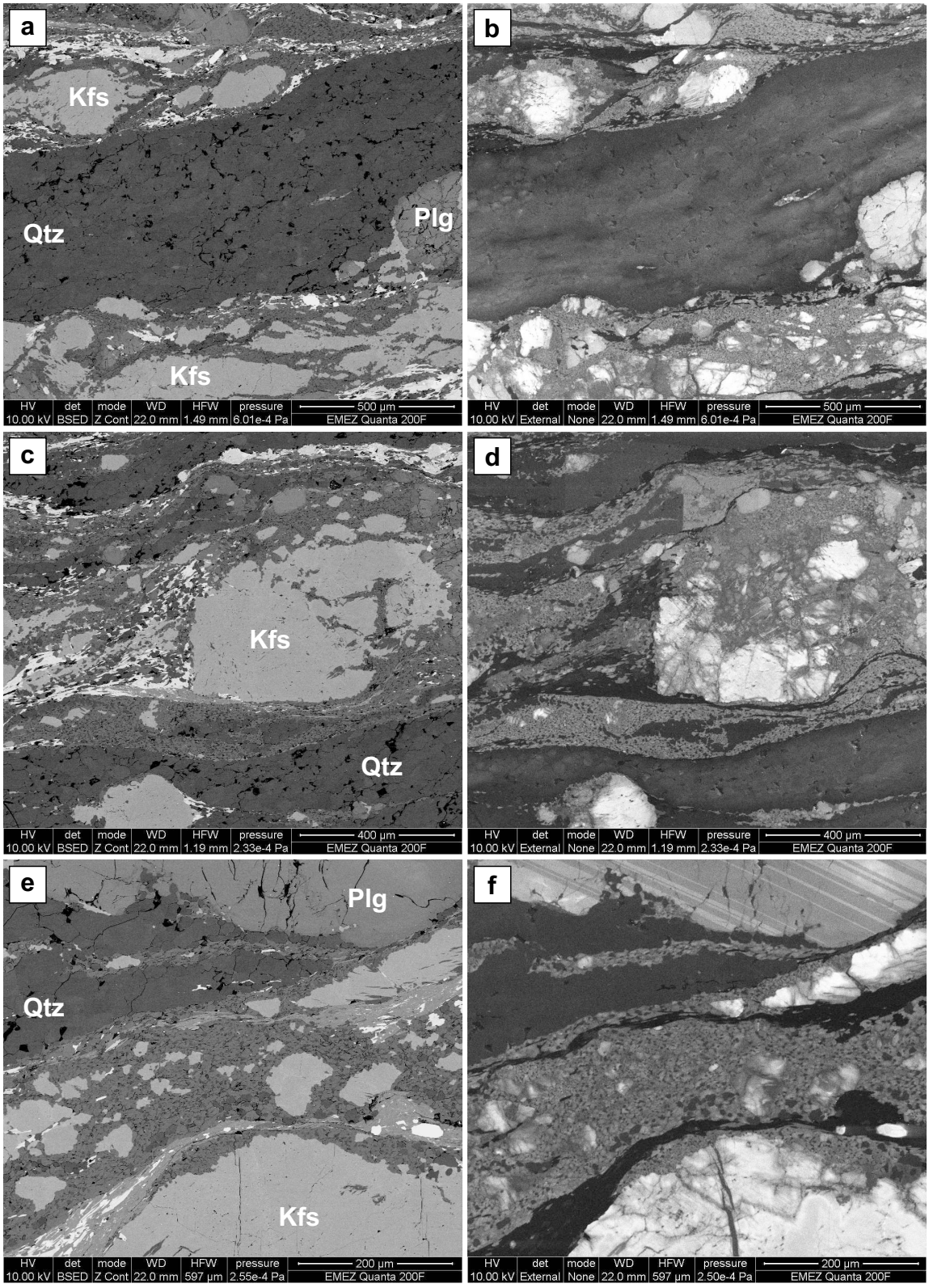
a
Kfs
Qtz
Plg
Kfs
HV 10.00 kV | det BSED | mode Z Cont | WD 22.0 mm | HFW 1.49 mm | pressure 6.01e-4 Pa | 500 µm | EMEZ Quanta 200F
b
HV 10.00 kV | det External | mode None | WD 22.0 mm | HFW 1.49 mm | pressure 6.01e-4 Pa | 500 µm | EMEZ Quanta 200F
c
Kfs
Qtz
HV 10.00 kV | det BSED | mode Z Cont | WD 22.0 mm | HFW 1.19 mm | pressure 2.33e-4 Pa | 400 µm | EMEZ Quanta 200F
d
HV 10.00 kV | det External | mode None | WD 22.0 mm | HFW 1.19 mm | pressure 2.33e-4 Pa | 400 µm | EMEZ Quanta 200F
e
Plg
Qtz
Kfs
HV 10.00 kV | det BSED | mode Z Cont | WD 22.0 mm | HFW 597 µm | pressure 2.55e-4 Pa | 200 µm | EMEZ Quanta 200F
f
HV 10.00 kV | det External | mode None | WD 22.0 mm | HFW 597 µm | pressure 2.50e-4 Pa | 200 µm | EMEZ Quanta 200F

Figure SOM3

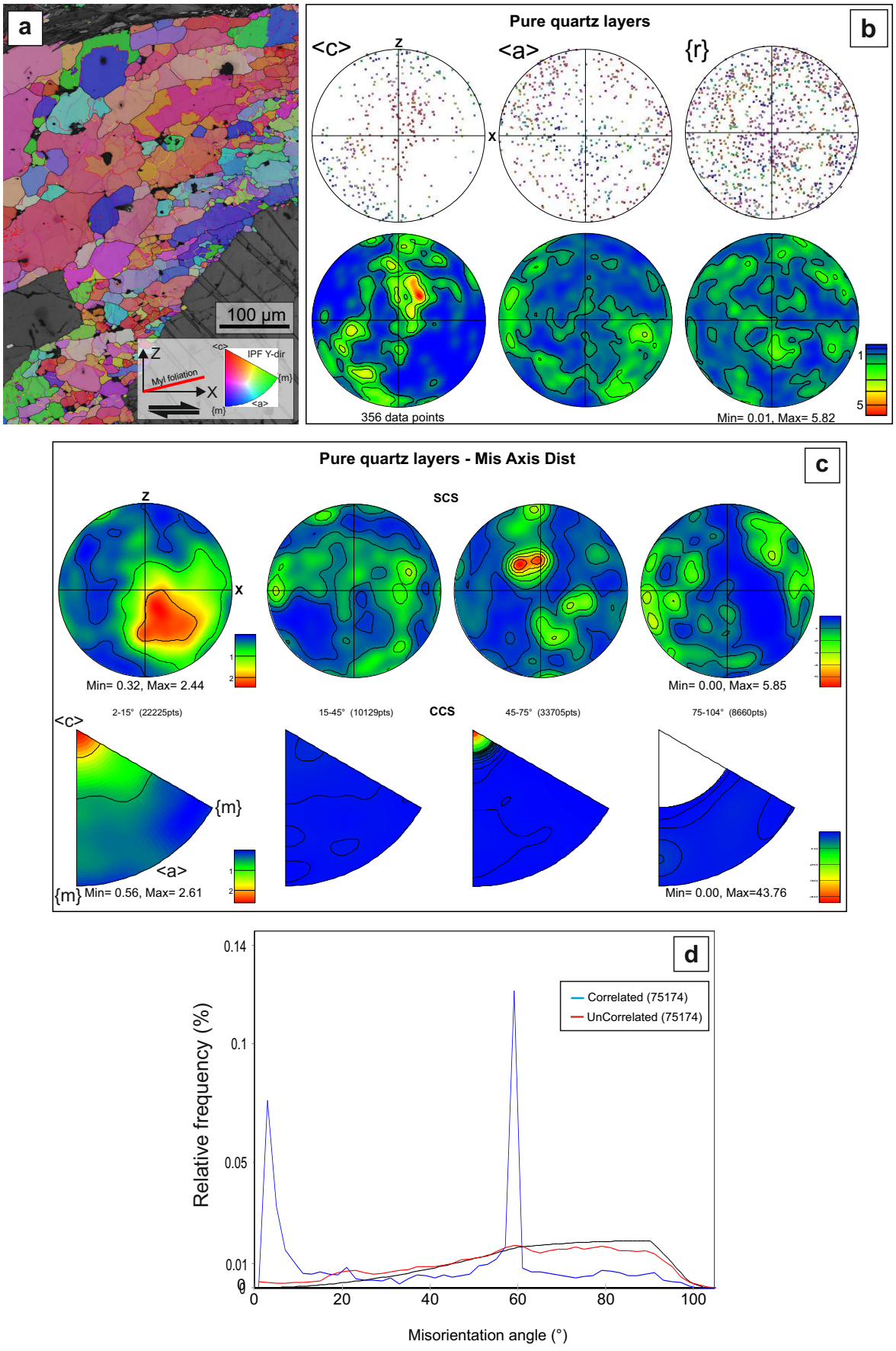
a
100 µm
Z
X
Myl foliation
IPF Y-dir
<c>
{m}
<a>
b
Pure quartz layers
<c>
z
<a>
x
{r}
356 data points
Min= 0.01, Max= 5.82
1
5
c
Pure quartz layers - Mis Axis Dist
SCS
z
x
Min= 0.32, Max= 2.44
Min= 0.00, Max= 5.85
2-15° (22225pts)
15-45° (10129pts)
CCS
45-75° (33705pts)
75-104° (8660pts)
<c>
{m}
<a>
{m}
Min= 0.56, Max= 2.61
Min= 0.00, Max=43.76
d
Correlated (75174)
UnCorrelated (75174)
Relative frequency (%)
0.14
0.1
0.05
0.01
0
0
20
40
60
80
100
Misorientation angle (°)

Figure SOM4

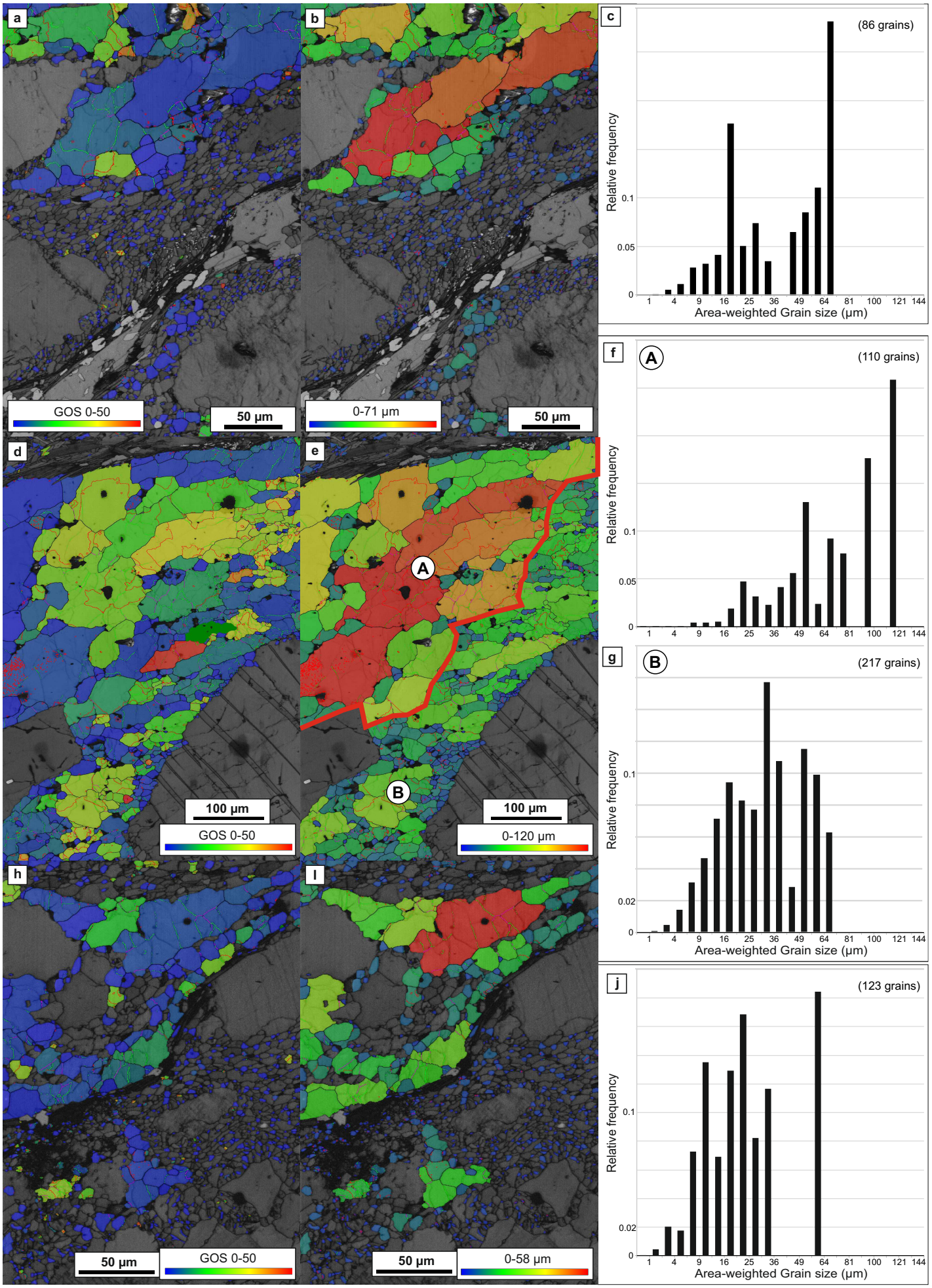
a
GOS 0-50
50 µm
b
0-71 µm
50 µm
c
(86 grains)
Relative frequency
0.1
0.05
0
1 4 9 16 25 36 49 64 81 100 121 144
Area-weighted Grain size (µm)
d
100 µm
GOS 0-50
e
A
B
100 µm
0-120 µm
f
A
(110 grains)
Relative frequency
0.1
0.05
0
1 4 9 16 25 36 49 64 81 100 121 144
g
B
(217 grains)
Relative frequency
0.1
0.02
0
1 4 9 16 25 36 49 64 81 100 121 144
Area-weighted Grain size (µm)
h
50 µm
GOS 0-50
i
50 µm
0-58 µm
j
(123 grains)
Relative frequency
0.1
0.02
0
1 4 9 16 25 36 49 64 81 100 121 144
Area-weighted Grain size (µm)

Figure SOM5

Figure SOM1. Grain Orientation Spread (GOS) maps for areas reported in Figs. 4 showing the average orientation spread for each grain of plagioclase (a), quartz (b) and K-feldspar (c) in the related frequency histograms. For (a) two misorientation profile across plagioclase subgrains are reported to show the limited internal distortion of plagioclase grains and the abrupt change in orientation across the analysed subgrain boundary.

Figure SOM2. EBSD orientation maps for K-feldspar and plagioclase. (a) Orientation map for K-feldspar of Fig. 3. (b) Pole figures reporting the crystallographic orientation of K-feldspar porphyroclasts and tails. (c) Misorientation axis distributions in sample (upper row) and crystal (lower raw) coordinate system for porphyroclasts and tails. (d) Pole figures reporting the crystallographic orientation of K-feldspar porphyroclast and fine-grained K-feldspar aggregate in the strain shadow (Area D Fig. 4). (e) Misorientation axis distributions in sample (upper row) and crystal (lower row) coordinate system for fine-grained K-feldspar aggregate. (f) Grain size distribution for the fine-grained K-feldspar aggregate. (g) Orientation map for Plagioclase and (h) K-feldspar. (i) Pole figures reporting the crystallographic orientation of plagioclase porphyroclast. (j) Pole figures reporting the crystallographic orientation of K-feldspar tail.

Figure SOM3. Backscattered and Cathodoluminescence images of Rieserferner mylonites. (a) BSE image of pure quartz layers (Qtz) between two sheared K-feldspar-myrmekite (Kfs) aggregate. (b) CL image of (a). Note the homogeneous signature of quartz and the complex microstructure of K-feldspar aggregate. (c) BSE image of a K-feldspar aggregate enveloped by sheared myrmekite. The top-left corner of the K-feldspar grain is reported in the map of Fig. 3. (d) CL image of (c). Note the complex microstructure of K-feldspar aggregate. (e) K-feldspar aggregate and sheared myrmekite. (f) CL image of (e).

Figure SOM4. EBSD orientation data and mapping for pure quartz layers. **(a)** Orientation map colour coded according to the inverse pole figure for Y-direction reported in the lower right corner. **(b)** Area-weighted grain size distribution for pure quartz layer. **(b)** Pole figures for quartz [c], <a> and {r} crystallographic elements. **(c)** Misorientation axis distributions in sample (upper row) and crystal (lower row) coordinate system. **(d)** Misorientation angle distribution for quartz.

Figure SOM5. Grain size and GOS maps for EBSD maps reported in Fig. 4, SOM2, 3, respectively, and relative quartz grain size distributions. (a) (b) (c) Grain size, GOS maps and grain size distribution for map reported in Fig. 5. (d) (e) (f) (g) Grain size, GOS maps and grain size distribution for map reported in Fig. SOM2. (h) (i) (j) Grain size, GOS maps and grain size distribution for map reported in Fig. 3.